

# Comparison of Gas- and Liquid-Phase Polymerization of Propylene with Heterogeneous Metallocene Catalyst

G. B. MEIER, G. WEICKERT, W. P. M. VAN SWAAIJ

Industrial Polymerization Processes, Process Technology Institute Twente, University of Twente, P.O. Box 217, 7500 AE Enschede, The Netherlands

Received 8 February 2000; accepted 22 September 2000

**ABSTRACT:** Sorption measurements are executed to study the sorption behavior of propylene in a semicrystalline polymer. Decreasing values for the Flory–Huggins interaction parameter with increasing temperature are obtained. Large deviations are found, especially at higher temperatures, compared to data from the literature. Propylene is polymerized in liquid and gaseous propylenes with  $\text{Me}_2\text{Si}[\text{Ind}]_2\text{ZrCl}_2/\text{MAO}/\text{SiO}_2$  as the metallocene catalyst. Lower relative reaction rates are found in the gas phase compared to the experiments in the liquid phase. The activation energies from the experiments in both phases are on the same order of magnitude. However, the literature versus experimental sorption data has a large effect on the determined kinetic parameters. © 2001 John Wiley & Sons, Inc. *J Appl Polym Sci* 81: 1193–1206, 2001

**Key words:** propylene polymerization; monomer sorption; gas phase; liquid phase; polymerization kinetics; metallocene catalyst

## INTRODUCTION

In comparison with the conventional Ziegler–Natta catalyst systems, metallocene catalysts offer a higher versatility and flexibility for the synthesis and control of polyolefin polymers. Despite all the development efforts in the area of synthesis of new catalyst compounds, few experimental studies are found in the open literature concerning the kinetic behavior of these metallocene systems at relevant process conditions. The kinetic data for gas- and liquid-phase (i.e., liquid propylene) polymerizations are especially scarce. Moreover, only a few studies are known in which the kinetics in both phases are compared. For modern propylene polymerization processes,

which contain liquid- and gas-phase steps, heterogeneous catalysts are required to obtain polymer particles with a narrow particle size distribution and high bulk density. However, it is well known that the catalyst behavior depends on the carrier and the supporting technique. In general, lower activities and higher molecular weights were found using heterogeneous analogues.

Propylene polymerization with a heterogeneous catalyst is a complex process involving chemical and physical effects. In order to reach the active centers, monomer molecules have to absorb into the amorphous part of the semicrystalline material and then diffuse to the active centers. On the kinetic level, the reaction is based on the rates of activation, propagation, and deactivation processes, which are all dependent on various process conditions. However, the reaction mechanism is independent of the reaction phase; the local polymerization rate depends on the local reaction conditions like the temperature and monomer concentration. Hutchinson and Ray<sup>1</sup>

Correspondence to: G. Weickert (g.weickert@ct.utwente.nl).  
Contract grant sponsor: BRITE-EURAM Project CATA-POL; contract grant number: BE 96-3022.

*Journal of Applied Polymer Science*, Vol. 81, 1193–1206 (2001)  
© 2001 John Wiley & Sons, Inc.

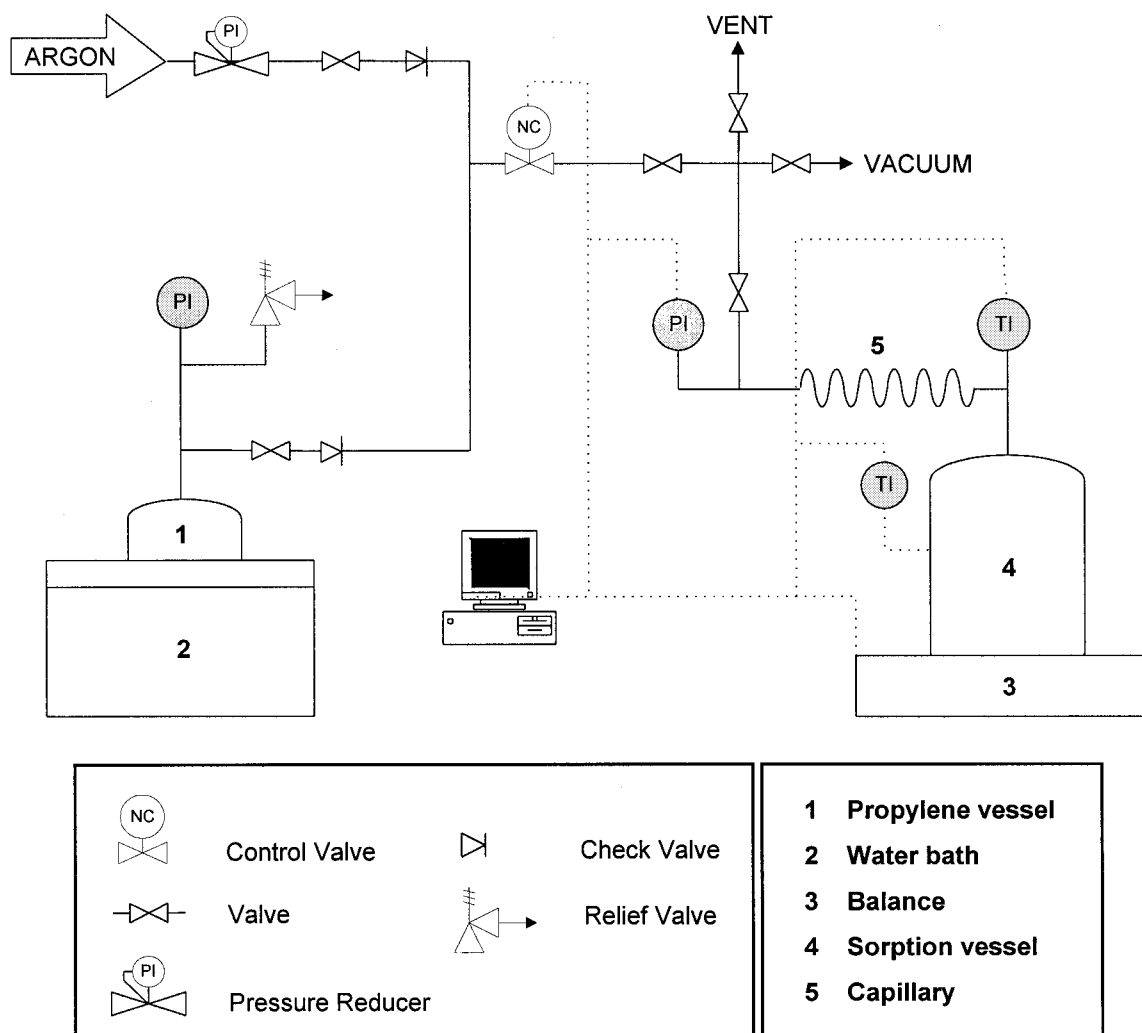


**Figure 1** The experimental setup for the sorption measurements.

and Samson et al.<sup>2</sup> showed that the kinetics can be unified by calculating the monomer concentration on the basis of polymer solution thermodynamics.

This article reports the results from gas- and liquid-phase polymerizations using *rac*-Me<sub>2</sub>Si[Ind]<sub>2</sub>ZrCl<sub>2</sub>/MAO/TIBA/silica (Grace) as a catalyst system. Sorption experiments were carried out to determine the monomer concentration near the active center. The results of the kinetic experiments were compared to check whether the kinetics were independent of the reaction phase.

## EXPERIMENTAL

### Sorption of Propylene

The sorption of propylene into polypropylene was measured using a gravimetric method. By adding

propylene gas to a vessel filled with polypropylene, the increment of the weight was used to calculate the sorption of propylene in the amorphous part of the semicrystalline material (Fig. 1). The sorption vessel (Fig. 1, part 4), which had a volume of 218 mL, was filled with 75 g of polymer and was placed on a balance (Fig. 1, part 3). All tubes containing propylene gas were electrically traced to prevent condensation. The temperature inside the sorption vessel, which was also heated electrically, was controlled with a Eurotherm PID controller. To reduce any manual handling during the measurements, an actuated valve was installed to add the propylene automatically. Before starting the addition of propylene, the sorption vessel was evacuated for 1 h. Prior to the addition of propylene, the weight of the vessel was measured and monitored for 0.5 h to ensure

**Table I Characteristics of Polymer Used for Sorption Experiments**

Polymer	Density (g/mL)	Crystallinity (%)	Porosity (%)
Prior to measurements	0.91	43.5	22
After experiments	0.91	43.7	20

that the balance was stabilized. After stabilization, the computer started the propylene addition by opening the actuated valve. The valve was closed when the desired pressure was reached. After the propylene addition the computer program waited until the pressure, temperature, and sample mass were stabilized and saved the data to disk. The procedure necessary to calculate the sorption data is given in the Appendix.

#### Polymer Sample Characterization

The polymer used for the sorption experiments was a product of a liquid pool experiment at 60°C using the same catalyst system used for the present kinetic measurements (see below). The density (pores excluded), crystallinity, and porosity were determined (Table I). The porosity was determined by mercury intrusion, considering a pore size between 0.1 and 10  $\mu\text{m}$ . To verify that these characteristics did not change during the experiments, the product was analyzed before and after the experiments. We concluded from the DSC curves that the crystallinity did not change in the entire range in which the measurements were executed.

#### Experimental Setup for Liquid Propylene Polymerizations

Liquid-phase polymerizations were performed in the same setup used by Samson et al.<sup>3</sup> The setup comprised a 5-L jacketed reactor; a catalyst injection system; and purification systems for propylene, hydrogen, nitrogen, and hexane. Additionally, the reactor was equipped with a helical stirrer and a sampling system.<sup>4</sup> Batch experiments were carried out under isothermal conditions. The reaction rate was determined by a calorimetric method assuming a constant heat transfer coefficient during the experiment.

#### Experimental Setup for Gas-Phase Polymerizations

The experimental setup for the gas-phase polymerizations is schematically shown in Figure 2.

The setup is based on the setup described by Samson et al.<sup>2</sup> Some adjustments were carried out in order to operate at higher pressures and to handle a different catalyst. The setup consisted of a stainless steel 0.5-L Büchi reactor for pressures up to 40 bar, a catalyst injection system, a small vessel to inject a certain amount of hydrogen, an evaporation vessel, and a temperature control system.

By keeping the temperature and pressure constant during the experiment, the reaction rate could be calculated from the feed rate required to keep the reactor pressure constant. Propylene gas, which was evaporated in the evaporation vessel, was fed into the reactor via a traced mass flow controller. The liquid propylene in the evaporator was kept at a temperature of 70°C to execute experiments up to 25 bar. To prevent condensation of propylene, all tubes of the monomer feed system were traced at 85°C.

A special helical stirrer was used to enforce good mixing inside the reactor. Moreover, 50 g of inert sodium chloride were used for every experiment to prevent catalyst particles from sticking to each other and to the reactor wall. The sodium chloride also improved the heat transfer from the reacting particles to the reactor wall. The stirrer forced the powder mixture to move upward along the reactor wall and downward along the stirrer shaft under the influence of gravity. A lower propeller stirrer was mounted to stir up the powder on the bottom of the reactor. The temperature inside the reactor, which was used to control the temperature within 0.1°C, was measured just above the stirrer but in direct contact with the powder flow.

A new catalyst injection system was developed to inject the dry catalyst powder. The catalyst was prepared under a nitrogen atmosphere in a glove box and mixed with 50 g of sodium chloride. Local high concentrations of catalyst in the reactor, which may lead to local hot spots, were avoided in this way. The catalyst mixture was placed in an injection vessel, which was connected to the reactor setup. Shortly before start-up, the catalyst mixture was injected via a valve into the evacuated reactor. After the experiment the injection vessel was checked for catalyst losses, but they were never found.

#### Catalyst System

The metallocene catalyst used for the gas- and liquid-phase polymerizations was  $\text{Me}_2\text{Si}[\text{Ind}]_2$ -

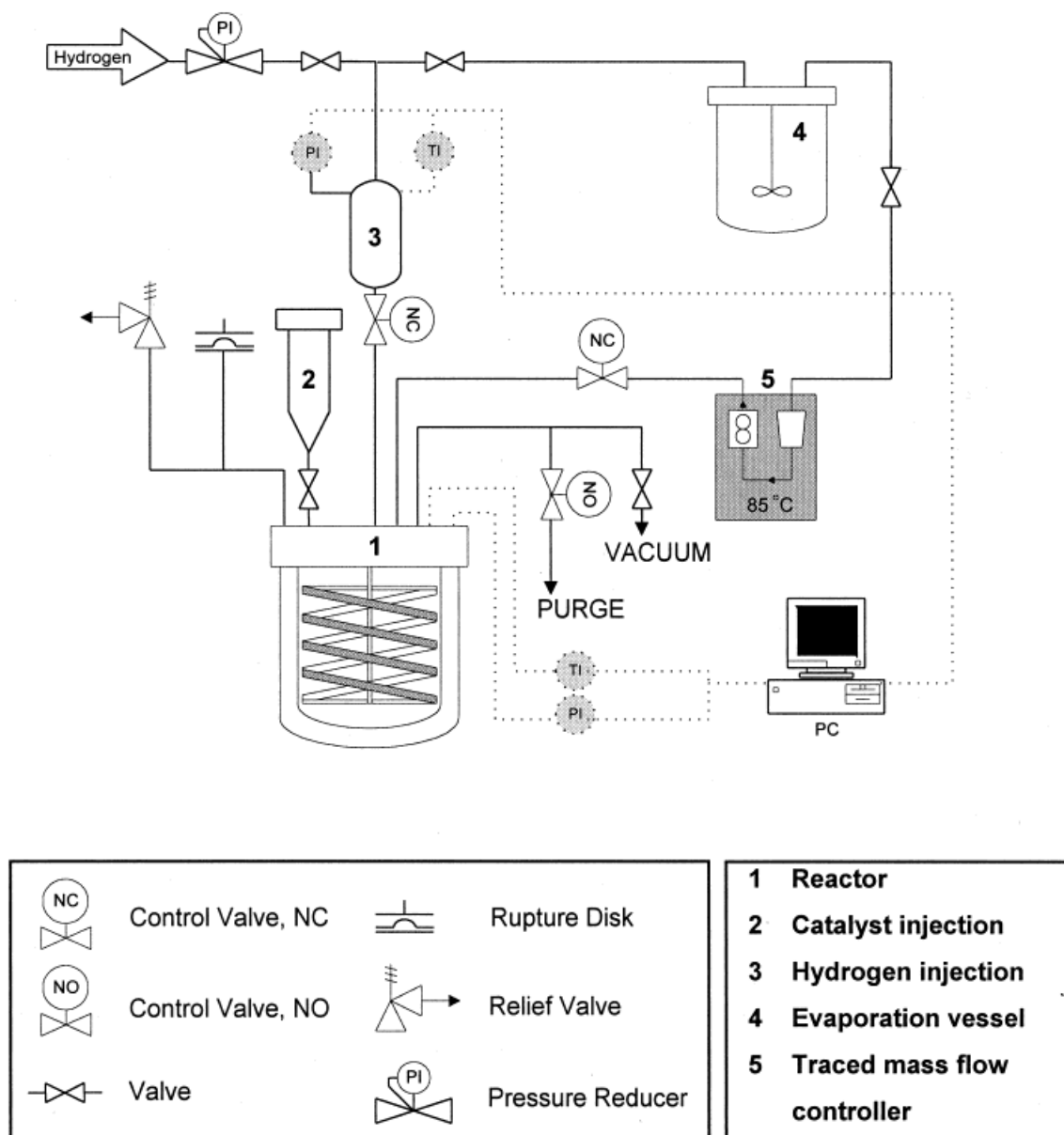


**Figure 2** The experimental setup for the gas-phase polymerizations.

ZrCl<sub>2</sub> (Fig. 3). Two groups<sup>5,6</sup> studied the polymerization behavior of this well-known system. Spaleck et al.<sup>5</sup> reported a rather low molecular weight (36,000 g/mol) of the polymer obtained after polymerization in liquid propylene at 70°C in the absence of hydrogen. Bonini et al.<sup>7</sup> studied the heterogeneous analogue in slurry at low pressure (2 bar) and low temperature (40°C). The system used for this study, was kindly supplied by Witco Co. (Bergkamen, Germany). It was supported on Grace silica with a concentration of 1 wt %. The MAO/SiO<sub>2</sub> support used for immobilization of the metallocene contained 25 wt % of alumina, giving

an [Al]/[Zr] ratio of 386. The average particle size of the silica used (SD3216-30, 10–110 μm) was 51 μm. A SEM photo of the morphological structure of one catalyst particle is given in Figure 4.

It is well known that the polymerization rate can be substantially increased by adding small amounts of aluminum alkyls,<sup>7</sup> especially triisobutylaluminum (TIBA). To be able to compare the results of gas- and liquid-phase experiments, the catalyst was precontacted with TIBA (Akzo Nobel) for 30 min prior to injection. The amount of TIBA used for precontacting was kept constant, resulting in a total [Al]/[Zr] ratio of 750.

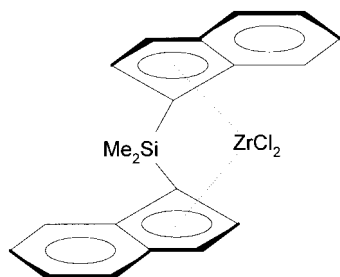


**Figure 3** The catalyst used for the kinetic experiments in the liquid and gas phases.

### Liquid-Phase Polymerization Procedure

Before each experiment the evacuated reactor was filled with 1 L of liquid propylene and heated to 60°C. Next, 200 mg of TIBA was injected to scavenge all impurities. After 1 h of stirring at 1000 rpm, the reactor content was purged through the drain. Then the prescribed amount of hydrogen and 2.6 L (at 20°C) of liquid propylene were added. The hydrogen concentration in the gas cap above the liquid ( $C_{H_2}^L$ ) at the reaction conditions was found by calculating the volume of this gas cap and compensating for the amount sorbed into the liquid propylene. Mizan et al.<sup>8</sup> reported the solubility of hydrogen in liquid propylene and found a Henry type of sorption, which is described in eq. (1).

$$C_{H_2}^L = k_H P_{H_2} \quad (1)$$

where  $k_H$  is the Henry coefficient and  $P_{H_2}$  is the partial pressure of hydrogen.

Table II presents relevant data for calculation of the hydrogen concentration in the gas cap of the liquid-phase reactor. The data on the density of liquid propylene and the vapor density were taken from the VDI-Wärmeatlas.<sup>9</sup>

The reactor content was brought to the desired temperature before catalyst injection. The temperature of the reactor and the coolant at the inlet and outlet of the reactor jacket were measured every 20 s during the experiment. The calorimetric method introduced by Samson et al.<sup>3</sup> was used to calculate the reaction rate in time. After 75 min the reaction was terminated by fast purging of the reactor. Due to evaporation of the liquid propylene, the temperature dropped rapidly and reduced the amount of polypropylene produced during the nonisothermal phase. The obtained polymer product was removed from the reactor and dried under a vacuum overnight.

### Gas-Phase Polymerization Procedure

Before each experiment the reactor was heated to 90°C under a vacuum for 30 min followed by flushing with nitrogen. The reactor was then brought to the desired temperature. The hydrogen injection vessel was pressurized with the desired amount of hydrogen. To prevent initial direct contact of the catalyst with pure hydrogen, the hydrogen injection vessel was pressurized with propylene up to 9 bar. Then the catalyst-salt mixture was injected into the evacuated reactor. A computer program written in HP VEE started the filling of the reactor to the desired pressure. The operation was simplified to a large extent because of the automation of the setup. During the reaction the operator controlled the setup from outside a concrete bunker. The reaction rate was obtained by measuring the monomer mass flow required to keep the pressure constant during the experiment. After 60 min the reactor content was purged to stop the reaction. The polymer product was washed with water to separate the sodium chloride and dried under a vacuum overnight.

### Sorption Theory

When the amount of sorbed monomer is sufficiently small (i.e., low monomer-polymer interaction), Henry's law can be used to describe the sorption in the amorphous part of a semicrystalline polymer.

$$c_m = k_H P \quad (2)$$

The volume fraction ( $\phi$ ) of penetrant inside the amorphous part can be calculated with

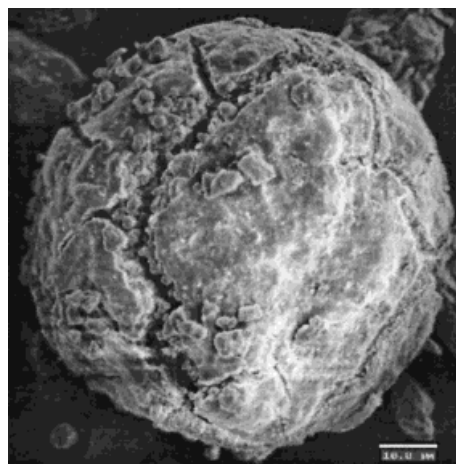


**Figure 4** An SEM photo of the catalyst morphology.



**Table II** Relevant Data Required to Calculate Hydrogen Concentration in Gas Cap of Liquid-Phase Reactor

$T$ (°C)	$k_H$ (mol/L bar)	$\rho_G$ (kg/m <sup>3</sup> )	$C_m^L$ (kg/m <sup>3</sup> )	$V_G$ (L)	$V_L$ (L)
40	0.0205	33.96	475.50	2.39	2.61
50	0.0245	43.18	454.58	2.32	2.68
60	0.0289	55.27	431.00	2.23	2.77
70	0.0334	72.98	403.17	2.13	2.87

$$\phi = \frac{k_H P M_m}{C_m^L} \quad (3)$$

At higher monomer concentrations, the interaction between the monomer and polymer increases. For this situation the Flory–Huggins equation is often used.

$$\ln \frac{P}{P^0} = \ln \phi + (1 - \phi) + \chi(1 - \phi)^2 \quad (4)$$

where  $P$  and  $P^0$  are the partial pressure and saturation pressure of the monomer, respectively; and  $\chi$  is the Flory–Huggins interaction parameter.

Samson et al.<sup>3</sup> estimated  $\chi$  with the Laar–Hildebrand equation.<sup>10</sup>

$$\chi = \frac{\nu_m}{RT} (\delta_m - \delta_p)^2 + \chi_s \quad (5)$$

where  $\nu_m$  is the molar volume of the monomer;  $R$  is the gas constant;  $T$  is the temperature;  $\delta_m$  and  $\delta_p$  are the solubility parameters of the monomer and polymer, respectively; and  $\chi_s$  is the correction for entropic interaction.

The  $\delta$  is a function of temperature, but  $\nu_m/R(\delta_m - \delta_p)^2$  and  $\chi_s$  are often nearly independent of the temperature.<sup>11</sup> Therefore, the Flory–Huggins parameter should decrease with increasing temperature according to eq. (6), which is in contrast to Samson et al.<sup>3</sup>

$$\chi = \frac{A}{T} + B \quad (6)$$

Moreover, the Flory–Huggins parameter may depend on the concentration, depending on the interaction between the solvent, amorphous, and crystalline part of the polymer. The Flory–Huggins equation appears to be very useful when

used as a correlative method, but it cannot be used in a predictive way if reasonable accuracy is required. Various experimentilists, for example, Favre et al.,<sup>12</sup> concluded that the Flory–Huggins interaction parameter remains an empirical fitting parameter.

The monomer concentration inside the polymer used for kinetic modeling was estimated by the following equation:

$$C_m = \phi \cdot C_m^L \quad (7)$$

where  $C_m^L$  is the concentration of liquid monomer for a given temperature.<sup>9</sup>

### Sorption of Hydrogen

It is well known that hydrogen not only influences the molecular weight of the polymer product but also affects the polymerization kinetics. Knowledge of the sorption behavior of hydrogen as a function of process conditions is therefore as important as monomer sorption behavior. However, for sparingly soluble penetrants the sorption can be described by Henry's law. For our system the situation was more complicated, because large amounts of propylene were sorbed into the amorphous part of the semicrystalline material. If Henry's law is still valid for the sorption of hydrogen in a polymer matrix swollen with propylene, polymerization experiments in the liquid phase should be executed with the same amount (mol %) of hydrogen in the gas cap as in the gas-phase experiments when the results are to be compared at a later time.

### Kinetic Model

The propagation rate is dependent on the monomer concentration and the number of active sites. For propylene polymerizations with zirconocenes at low monomer concentration, the reaction order with respect to monomer concentration was re-

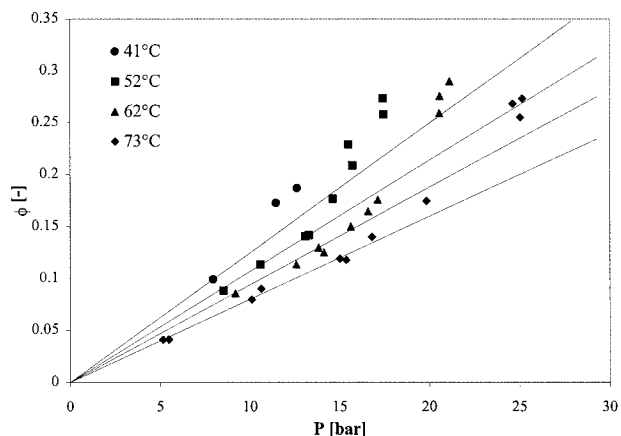


**Figure 5** The fitting of the sorption measurements with Henry's law.

ported to be higher than one [see eq. (8)].<sup>13,14</sup> Fait et al.<sup>15</sup> postulated a kinetic model based on the presence of a single-center, two-state catalyst system in which both states had different propagation rates. According to the proposed mechanism, interconversion between the two states leads to a lower concentration of the slow state at higher monomer concentration, leading to an overall order of reaction in the monomer of larger than one.

$$R_p = k_p C^* C_m^n \quad (1 < n < 2) \quad (8)$$

where  $R_p$  is the reaction rate,  $C^*$  is the number of active centers per gram of catalyst,  $n$  is the reaction order, and  $C_m$  is the monomer concentration based on the sorption equations presented before. In the simple power law in eq. (8)  $k_p = k_{p,0} \exp[-(E_{act,p}/RT)]$ , where  $k_p$  is the propagation rate constant and  $E_{act,p}$  is the activation energy for propagation.

The decay in polymerization rate generally observed after the buildup period is intensively discussed in the literature. It is generally believed<sup>16</sup> that this loss of activity in time cannot be explained by an intraparticle monomer diffusion limitation through the growing polymer layer. Most of the experimental results can be analyzed according to a decreasing number of active centers with time due to chemical deactivation. We chose to describe the deactivation by the following simple first-order relation:

$$\frac{dC^*}{dt} = -k_d C^* \quad (9)$$

where  $t$  is time,  $k_d$  is the deactivation constant,  $E_{act,d}$  is the activation energy for deactivation, and  $k_d = k_{d,0} \exp[-(E_{act,d}/RT)]$ .

Integration of eq. (9) leads to the number of active sites as a function of time.

$$C^* = C_{max}^* \exp(-k_d t) \quad (10)$$

where  $C_{max}^*$  is the maximum number of active centers per gram of catalyst.

Substitution into eq. (8) leads to

$$R_p = k_p C_m C_{max}^* \exp(-k_d t) = R_{p,max} \exp(-k_d t) \quad (11)$$

where  $R_{p,max}$  is the maximum reaction rate. Note that eq. (11) is valid after the buildup period.

## RESULTS

### Sorption Measurements

The propylene sorption experiments were performed at different temperatures (41, 52, 62, and 73°C) and pressures (5–25 bar). Figure 5 presents the results of the sorption experiments, together with a best fit according to Henry's law. The results are summarized in Table III. These fits were only based on the sorption measurements at low volume fractions. The data at low volume fractions could be fitted with Henry's law, but failed for higher values.

The Flory–Huggins interaction parameter was determined for every data point. The error in the determined interaction parameter was about 5% for the measurements at 41°C and increased to about 9% for the measurements at 73°C. In Figure 6 each temperature series is fitted with an average value for the interaction parameter. In Figure 7 the experimental data are fitted using interaction parameters given by Samson et al.<sup>3</sup> The experimentally determined values and the literature values for the Flory–Huggins interac-

**Table III** Henry Constants at Different Temperatures Used to Fit Experimental Data at Low Volume Fractions

Temperature (°C)	$k_H$ (mol/L bar)	Temperature (°C)	$k_H$ (mol/L bar)
41	0.141	62	0.095
52	0.115	73	0.075

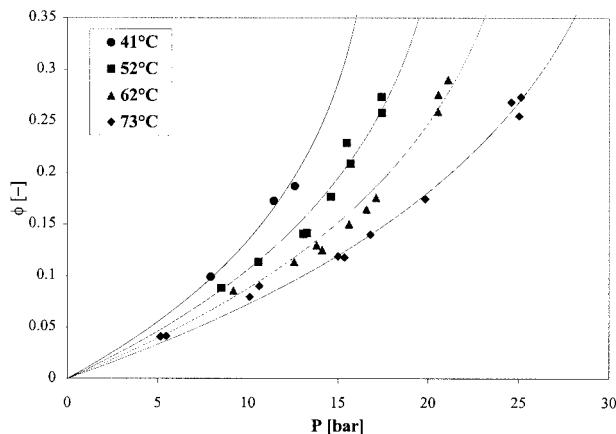


**Figure 6** The fitting measurements with the Flory–Huggins equation.

tion parameter are summarized in Table IV. The measured value for the Flory–Huggins interaction parameter decreased with increasing temperature whereas the values given by Samson et al.<sup>3</sup> dramatically increased with the temperature.

Based on eq. (6), a linear relation between the measured interaction parameter and the reciprocal temperature was expected (Fig. 8). Equation (12) represents the best fit.

$$\chi = \frac{730.43}{T} - 1.501 \quad (12)$$

All experiments were executed using the same polymer made in liquid propylene at 60°C with a heterogeneous metallocene catalyst. Care should be taken when using the absolute values, because

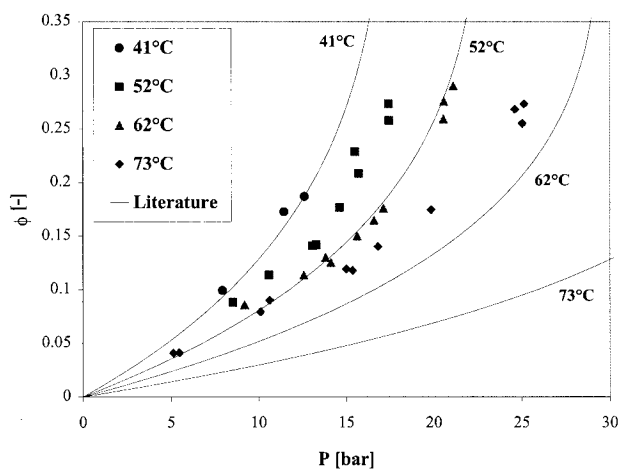


**Figure 7** A comparison of the sorption measurements with literature data.

**Table IV** Flory–Huggins Interaction Parameter as Function of Temperature: Literature Versus Experimental Data

Temperature (°C)	Interaction Parameter <sup>a</sup>	Average Measured Value
41	0.86	0.82
52	0.99	0.75
62	1.16	0.69
73	1.45	0.61

<sup>a</sup> Given by Samson et al.<sup>3</sup>

the Flory–Huggins interaction parameter may depend on the degree of crystallinity of the polymer.

## Liquid-Phase Experiments

### Influence of Al/Zr Ratio

The sensitivity towards the amount of TIBA was tested during three different experiments at different Al/Zr ratios (Fig. 9). All experiments were carried out at 60°C and with 2% hydrogen in the gas cap. The polymerization rate was calculated as the amount of polypropylene per gram of metallocene on the silica support per hour (kg/g<sub>met</sub> h). This was to later compare the results with catalysts with different metallocene loadings. The large initial fluctuations in polymerization activity did not depict real fluctuating reaction rates; they were caused by the PID controller. Although the temperature could be controlled within 0.2°C, the cooling water temperature did show some small oscillation in the beginning of an experi-

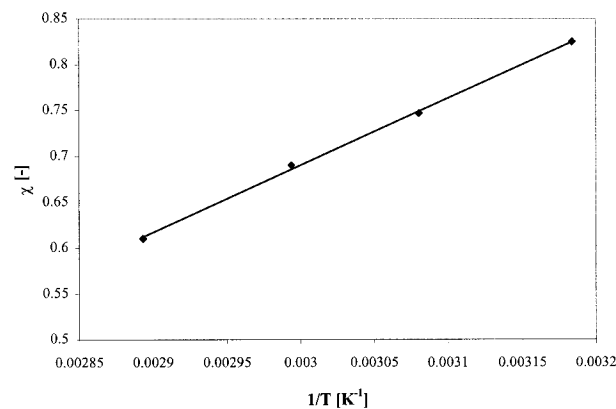


**Figure 8** The measured Flory–Huggins parameters versus the reciprocal temperature.



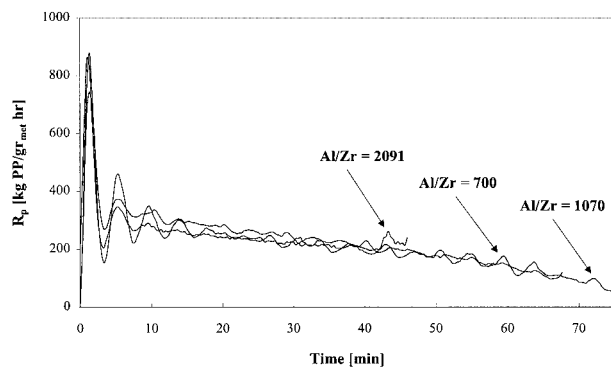


**Figure 9** The influence of the Al/Zr ratio on the polymerization rate during liquid-phase polymerization.

ment, which directly influenced the apparent polymerization rate. The experiments at different Al/Zr ratios showed only minor deviations from each other. This indicated that in this range a variation in the ratio did not have much influence on the polymerization rate.

#### Influence of Temperature

The influence of temperature on the reaction rate was studied by varying the temperature from 40 to 70°C (Fig. 10). Table V gives an overall summary of the experiments by presenting the reaction conditions and some fitted kinetic parameters. Note the large differences between the values for the monomer concentration based on theoretical literature sorption data and the values based on the measured sorption data, especially at higher temperatures. At 70°C the measured monomer concentration was about 4 times higher than the concentration calculated by Samson et al.<sup>3</sup>

The experiment at 70°C showed the presence of a critical polymer concentration after about 20 min (i.e., a propylene conversion above 40–50%), which caused a sharp decrease of the heat trans-

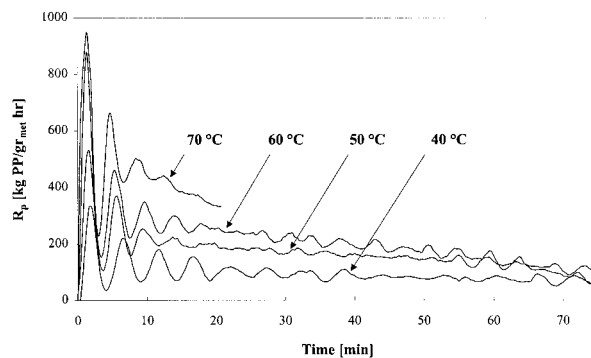


**Figure 10** The influence of the temperature on the polymerization rate during liquid-phase polymerizations.

fer coefficient manifest from the temperature recordings (see also Samson et al.<sup>3</sup>). The observed transition in the heat transfer was ascribed to the changing flow behavior of the reactor content.<sup>3</sup>

#### Influence of Hydrogen

The influence of hydrogen on the polymerization kinetics was investigated at 60°C in the liquid phase. Experiments were executed between 0 and 2.2% hydrogen in the gas cap. This relatively small range was chosen because the sensitivity of metallocene catalysts toward hydrogen, which is related to the molecular weight of the polymer, is large compared to classical Ziegler–Natta catalysts.<sup>17</sup> The  $R_{p,max}$  and  $k_d$  were determined by fitting the reaction rate curves to eq. (11). In Figures 11 and 12 the maximum reaction rate and deactivation constant are given as a function of the hydrogen concentration. A linear relation was obtained between the maximum reaction rate and the hydrogen concentration in the gas cap. No saturation effect was found for the range in which the experiments were executed, which was shown by Samson et al.<sup>18</sup> However, the increasing trend

**Table V** Summary of Liquid-Phase Experiments at Different Temperatures

$T$ (°C)	$H_2$ Gas Cap (mol %)	$H_2$ Liquid (mol %)	$C_m$ (kg/m <sup>3</sup> )		$R_{p,max}$ (kg PP/g <sub>met</sub> h)	$k_d$ (min <sup>-1</sup> )
			This Work	Samson et al. <sup>3</sup>		
40	2.45	0.028	208.8	200.3	125.8	0.0088
50	2.38	0.043	233.0	156.5	232.5	0.0096
60	2.22	0.064	257.9	111.0	377.5	0.0179
70	2.05	0.086	276.1	70.4	578.0	0.0266

PP, polypropylene.

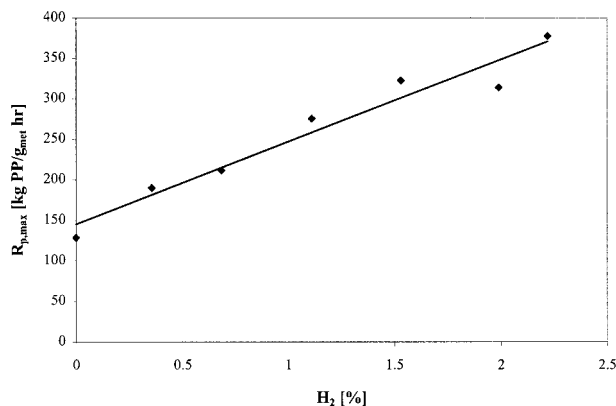


**Figure 11** The influence of hydrogen on the maximum polymerization rate.

for the deactivation constant with the hydrogen concentration, which was observed at higher hydrogen concentrations, was also found by Samson et al.<sup>18</sup> In general, a higher deactivation rate was observed at higher reaction rates, which was caused by either higher temperatures or hydrogen. No deactivation phenomena were found for the experiment without hydrogen that was associated with a low reaction rate.

Several possible explanations for the increased catalyst activity in the presence of hydrogen are given in the literature.<sup>5</sup> One possibility may be the shortcutting of slow propagation steps, which occurred after isolated secondary insertions (2–1 insertions).

## Gas-Phase Experiments

### Influence of Temperature

The influence of temperature on the polymerization rate was studied at temperatures between 40

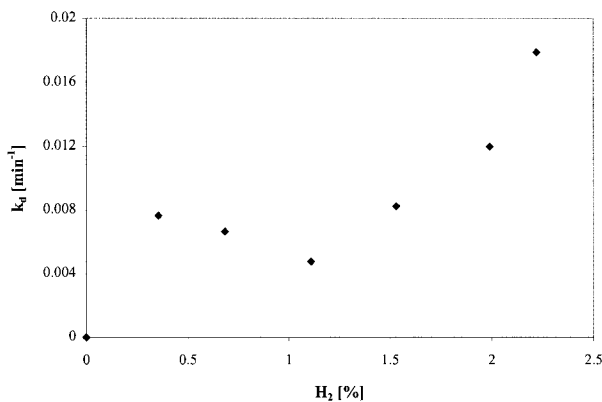


**Figure 12** The influence of hydrogen on the deactivation constant ( $k_d$ ).

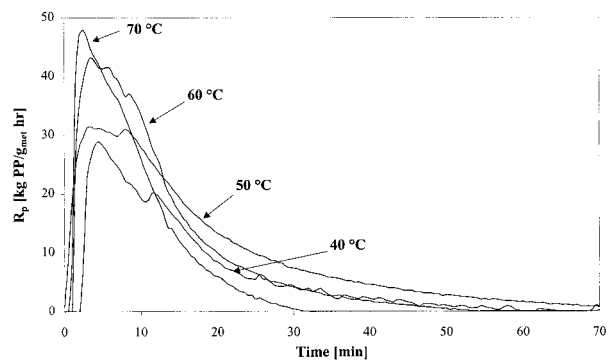


**Figure 13** The influence of the temperature on the polymerization rate during gas-phase polymerization at 10-bar pressure.

and 70°C at 10-bar pressure and 2 mol % of hydrogen. As can be seen in Figure 13, the reaction rate and the deactivation rate increased with increasing temperature. In contrast to the experiments in the liquid phase, the catalyst did not show activity directly after injection. Especially at lower temperatures, some time was required to reach maximum polymerization activity. The model presented earlier did not take any induction period or activation processes into account.

### Influence of Pressure

The influence of pressure was studied between 5 and 25 bar at 70°C. Figure 14 shows that the maximum reaction rate increased more or less in a linear fashion with the monomer concentration in the amorphous part of the polymer, reflecting the first-order reaction kinetics. The  $C_m$  was cal-

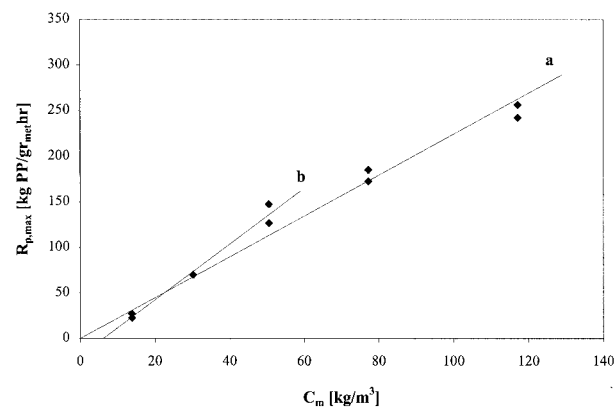


**Figure 14** The influence of the monomer concentration on the maximum polymerization rate during gas-phase polymerization at 70°C: (a) the fit of all data and (b) the fit at low concentrations (<15 bar).

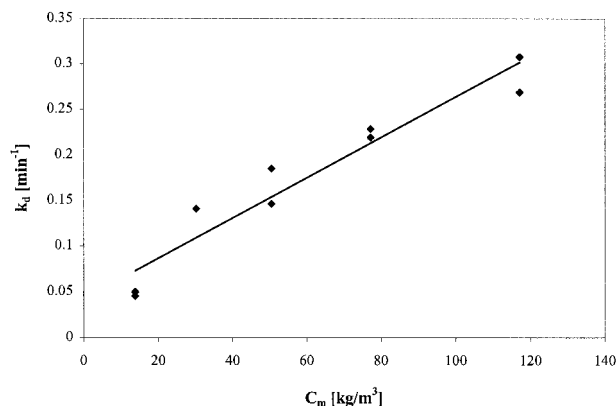


**Figure 15** The influence of the monomer concentration on the deactivation constant during gas-phase polymerization at 70°C.

culated according to the experimental sorption data presented in an earlier section. When fitting the data at low concentration (<15 bar), a trend line with an intercept not equal to zero was obtained (Fig. 14, plot b). This supported the theory of a reaction order of higher than one discussed before. Another possible explanation may have been a less accurate estimate of the monomer concentration at low pressures.

In Figure 15 the  $k_d$  is given as a function of the monomer concentration. Again a linear relation was obtained. According to the model, the deactivation rate should not depend on the monomer concentration; however, this dependency was found previously. Kohara et al.<sup>19</sup> also obtained a linear relation between the deactivation constant and the monomer concentration using a Ziegler-Natta catalyst.

### Comparison of Liquid- and Gas-Phase Polymerization Kinetics

The main difference between the gas- and liquid-phase experiments seemed to be the monomer concentration near the active center, if one assumed that the same reaction mechanism holds for both phases and the same relative polymerization rate should be obtained. Figures 16 and 17 present the Arrhenius plots of the gas- and liquid-phase experiments based on the measured and (theoretical) literature<sup>3</sup> sorption data, respectively. The constants for the kinetic model, which are based on both sorption data sets, are summarized in Table VI.

In general, lower relative reaction rates ( $R_{p,max}/C_m$ ) were found in the gas phase, which

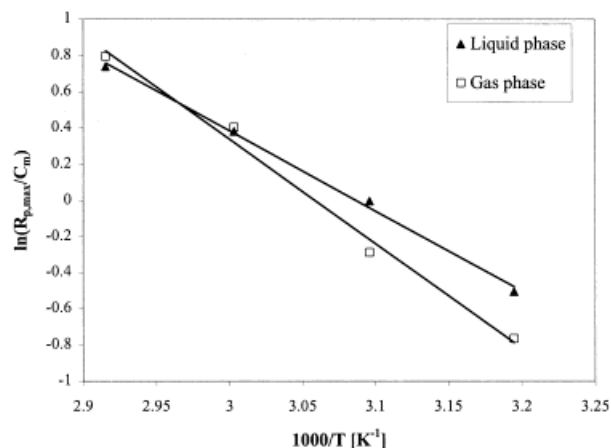


**Figure 16** Arrhenius plots (propagation) of gas- and liquid-phase experiments using the measured sorption data.

agreed with the results of Samson et al.<sup>2</sup> Our simplified kinetic model did not take activation of the catalyst into account, although a clear initial increase in polymerization activity was observed during all gas-phase experiments. The time required to reach the maximum polymerization activity for a gas phase experiment was about 3–5 min. In this time the deactivation processes were already influencing the polymerization rate, causing a lower maximum polymerization rate. This may explain the lower relative activity observed for the gas-phase experiments. An alternative method could be to use the initial reaction rate instead of the maximum polymerization rate by extrapolation to time zero. However, such extrapolations would lead to unrealistic values of the initial reaction rates. This effect was enhanced by

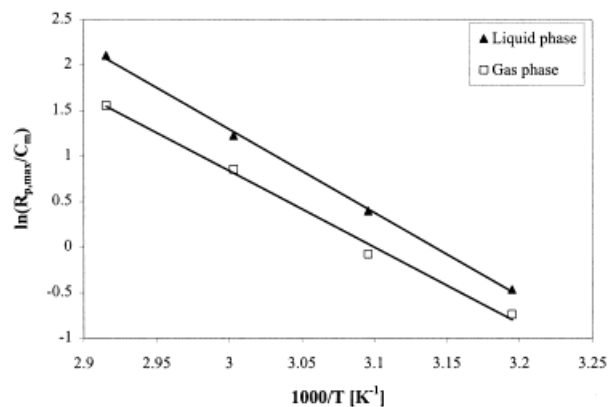


**Figure 17** An Arrhenius plot (propagation) of the gas- and liquid-phase experiments using the sorption data given by Samson et al.<sup>3</sup>

**Table VI** Constants for Kinetic Model for Gas- and Liquid-Phase Polymerizations

Sorption Data Set	Liquid Phase		Gas Phase	
	This Work	Samson et al. <sup>3</sup>	This Work	Samson et al. <sup>3</sup>
$k_{p,0}C_{\max}^*$ (m <sup>3</sup> /h g <sub>met</sub> )	$8.67 \times 10^5$	$3.17 \times 10^{12}$	$4.69 \times 10^9$	$1.94 \times 10^{11}$
$E_{\text{act},p}$ (kJ/mol)	36.8	76.2	48.0	69.7
$k_{d,0}$ (min <sup>-1</sup> )		$5.09 \times 10^3$		$7.95 \times 10^3$
$E_{\text{act},d}$ (kJ/mol)		35		31

the higher deactivation rate observed for the gas-phase experiments (Fig. 18). Samson et al.<sup>2</sup> also found higher deactivation rates during gas-phase polymerizations. An Arrhenius plot for the gas- and liquid-phase experiments based on the initial reaction rate is given in Figure 19.

The activation energies found for the liquid- and gas-phase experiments were on the same order of magnitude. However, the sorption data used (literature vs. experimental) had a large effect on the determined kinetic parameters. The temperature series in the liquid phase was unfortunately not executed at a completely constant hydrogen concentration in the gas cap. The concentration dropped from 2.45% at the lowest temperature to 2.05% at the highest temperature (Table V). The experiments in the liquid phase had a varying hydrogen concentration in the gas cap and showed that this variation in hydrogen concentration affects the maximum reaction rate. Thus, the determined activation energy for propagation for the liquid-phase experiments was in fact too low, being about 10%. This may explain the slightly lower activation energy (based on ex-

perimental sorption data) found for the liquid-phase experiments. However, the sorption behavior of hydrogen in a polymer may depend on the amount of propylene sorbed in the polymer. Such information may help to explain the differences between the gas- and liquid-phase kinetic data.

## CONCLUSIONS

The sorption data of propylene in polypropylene were measured using a gravimetric method. At low pressures the sorption could be described with Henry's law; at higher concentrations the Flory–Huggins equation appeared to be a useful fitting equation. The decreasing values of the Flory–Huggins parameter were measured with increasing temperature, which was in contrast to data given by Samson et al.<sup>3</sup> but in line with theoretical expectations. Polymerizations were executed in gaseous and liquid propylenes at different temperatures, pressures, and hydrogen

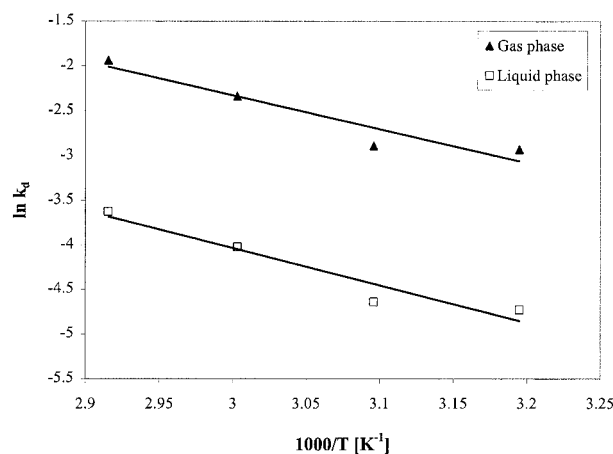


**Figure 18** An Arrhenius plot (deactivation) for the gas- and liquid-phase experiments.

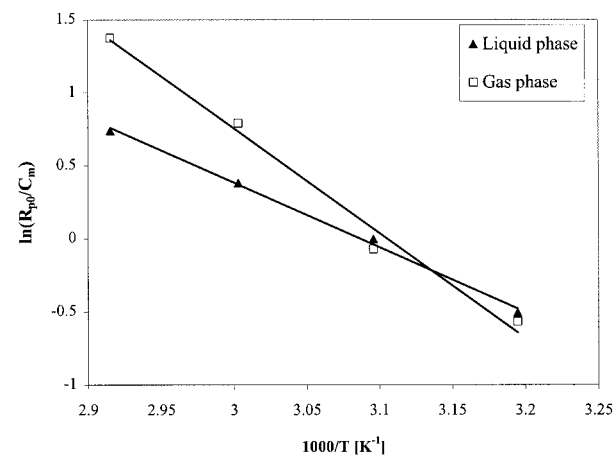


**Figure 19** An Arrhenius plot (propagation) of the gas- and liquid-phase experiments using the measured sorption data. The initial polymer reaction rate ( $R_{p,0}$ ) was determined by extrapolation to time zero.

concentrations. Hydrogen appeared to have a large influence on the reaction and deactivation rate. In general, a higher deactivation rate was observed at higher reaction rates, which was caused by either higher temperatures or hydrogen.

The influence of the monomer concentration was studied at 70°C in the gas phase. A reaction order above one was obtained at low concentrations of below 15 bar. This supported the theory of a single-center, two-state catalyst postulated by Fait et al.<sup>15</sup>

The sorption data of propylene were used to compare the results of the gas- and liquid-phase polymerizations. Lower relative reaction rates were found for gas-phase polymerizations. The activation energies found for the liquid- and gas-phase experiments were comparable. The sorption data used from the literature or experiments had a large effect on the estimated kinetic parameters.

Adequate monomer sorption data and hydrogen sorption data are both required for a correct comparison between gas- and liquid-phase kinetic data. Unfortunately, the sorption behavior of hydrogen in polypropylene swollen with propylene was unknown and difficult to determine exactly.

We gratefully acknowledge K. van Bree and F. ter Borg for the construction of the experimental setups and technical assistance. We also acknowledge G. H. Banis for his technical support and W. R. Smit, B. G. C. J. Wijers, and S. N. Kuper for their assistance in the experimental part.

## NOMENCLATURE

A	constant (K)
B	constant
$C^*$	number of active sites (mol/g <sub>met</sub> )
$c_m$	monomer concentration (mol/L)
$C_m$	monomer concentration (kg/m <sup>3</sup> )
$C_H$	hydrogen concentration (mol/L)
$E_{act}$	activation energy (J/mol)
$k_d$	deactivation rate constant (min <sup>-1</sup> )
$k_H$	Henry constant (mol/L bar)
$k_p$	propagation rate constant (m <sup>3</sup> /mol h)
$m$	mass (kg)
$M_m$	monomer molecular weight (kg/mol)
$P$	Partial pressure (bar)
$P^0$	saturation pressure (bar)
$R$	gas constant (J/mol K)
$R_p$	reaction rate (kg/g met h)

$t$	time (min)
$T$	temperature (K)
$V$	volume (m <sup>3</sup> )
$X$	crystallinity

## Greeks

$\chi$	Flory–Huggins interaction parameter
$\delta$	solubility parameter (J/mL) <sup>0.5</sup>
$\phi$	volume fraction
$\nu$	molar volume (cm <sup>3</sup> /mol)
$\rho$	density (kg/m <sup>3</sup> )

## Subscripts and Superscripts

$G$	gas phase
$H_2$	hydrogen
$L$	liquid phase
$m$	monomer
max	maximum condition
$n$	reaction order
$p$	polymer
$p$	polymerization or propagation
0	initial condition
s	entropic correction, see eq. 5

## Abbreviations

Al	aluminum
MAO	methylaluminoxane
TIBA	triisobutylaluminum
Zr	zirconium

## APPENDIX

### Calculation Procedure for Sorption Measurements

The weight increment ( $\Delta m$ ) from a sorption experiment was calculated from the measured mass before ( $m_1$ ) and after ( $m_2$ ) the addition of propylene gas ( $m_G, m_{sorbed}$ ).

$$\Delta m = m_2 - m_1 = m_G + m_{sorbed} \quad (\text{A.1})$$

The volume of the vessel ( $V_{vessel}$ ) was used to calculate the volume of the gas ( $V_G$ ) not sorbed in the amorphous part of the polymer, which is the gas between the polymer particles and the gas in the pores of the polymer ( $V_p$ ).



$$V_G = V_{\text{vessel}} - V_p = V_{\text{vessel}} - \frac{m_p}{\rho_p} \quad (\text{A.2})$$

Multiplying this volume by the gas density ( $\rho_G$ ) results in the mass of the gas ( $m_G$ ):

$$m_G = V_G \rho_G \quad (\text{A.3})$$

The volume of sorbed propylene ( $V_{\text{sorbed}}$ ) can be calculated using the density of liquid propylene.

$$V_{\text{sorbed}} = \frac{\Delta m - m_G}{C_m^L} \quad (\text{A.4})$$

The volume fraction ( $\phi$ ) of the monomer in the amorphous parts of the polymer ( $\phi_m$ ) can be calculated with

$$\phi = \frac{V_{\text{sorbed}}}{V_{\text{sorbed}} + V_{p,\text{amorph},0}} = \frac{V_{\text{sorbed}}}{V_{\text{sorbed}} + (1 - X)V_{p,0}} \quad (\text{A.5})$$

Swelling of the polymer results in an increase of the polymer volume:

$$V_p = V_{p,0} + V_{\text{sorbed}} \quad (\text{A.6})$$

The calculated polymer volume ( $V_p$ ) in turn changes the volume of the gas not sorbed into the polymer, which influences the volume fraction of monomer sorbed into the polymer, and so forth. This step must be repeated until the volume fraction  $\phi$  converges.

## REFERENCES

- Hutchinson, R. A.; Ray, W. H. *J Appl Polym Sci* 1990, 41, 51.
- Samson, J. J. C.; van Middelkoop, B.; Weickert, G.; Westerterp, K. R. *AIChE J* 1999, 45, 1548.
- Samson, J. J. C.; Weickert, G.; Heerze, A. E.; Westerterp, K. R. *AIChE J* 1998, 44, 1424.
- Shimizu, F.; Pater, J. T. M.; Weickert, G. *J Appl Polym Sci*, submitted.
- Spaleck, W.; Aulbach, M.; Bachmann, B.; Küber, F.; Winter, A. *Macromol Symp* 1995, 89, 237.
- Carvill, A.; Tritto, I.; Locatelli, P.; Sacchi, M. C. *Macromolecules* 1995, 30, 7056.
- Bonini, F.; Fraaije, V.; Fink, G. *J Polym Sci Part A Polym Chem* 1995, 33, 2393.
- Mizan, T. I.; Li, J.; Morsi, B. I.; Chang, M. Y.; Maier, E.; Singh, C. P. P. *Chem Eng Sci* 1994, 49, 821.
- VDI-Wärmeatlas, 6th ed.; VDI-Gesellschaft Verfahrenstechnik und Chemieingenieurwesen (GVC) Verlag, Düsseldorf: 1991.
- Barton, A. F. M. *CRC Handbook of Polymer-Liquid Interaction Parameters and Solubility Parameters*; CRC Press: Boca Raton, FL, 1990; p 284.
- Prausnitz, J. M.; Lichtenthaler, R. N.; de Azevedo, E. G. *Molecular Thermodynamics of Fluid-Phase Equilibria*, 2nd ed.; Prentice-Hall: Englewood Cliffs, NJ, 1986.
- Favre, E.; Nguyen, Q. T.; Schaezel, P.; Clément, R.; Néel, J. *J Chem Soc Faraday Trans* 1993, 89, 4339.
- Fink, G.; Herfert, N.; Montag, P. *Ziegler Catalysts*; Springer-Verlag: New York, 1995; p 159.
- Jüngling, S.; Mülhaupt, R.; Stehling, U.; Brintzinger, H. H.; Fischer, D.; Langhauser, F. *J Polym Sci Part A Polym Chem* 1995, 33, 1305.
- Fait, A.; Resconi, L.; Guerra, G.; Corradini, P. *Macromolecules* 1999, 32, 2104.
- Kim, I.; Woo, S. I. *Kor J Chem Eng* 1990, 7, 95.
- Blom, R.; Dahl, I. M. *Macromol Chem Phys* 1999, 200, 442.
- Samson, J. J. C.; Bosman, P. J.; Weickert, G.; Westerterp, K. R. *J Polym Sci Part A Polym Chem* 1999, 37, 219.
- Kohara, T.; Shinoyama, M.; Doi, Y.; Keii, T. *Makromol Chem* 1979, 180, 2139.